

# Viscous-Inviscid Matching for Surface-Piercing Wave-Body Interaction Problems

**J. A. Hamilton and R. W. Yeung**

Department of Mechanical Engineering

University of California at Berkeley

Berkeley, California 94720-1740, USA

*Corresponding E-mail: rwyung@socrates.berkeley.edu*

## 1 Introduction

In wave-body interaction problems encountered in many ocean-engineering applications, an open boundary that separates an area of interest from the rest of a semi-infinite domain is often present. Because phenomena of interest are usually located in the inner region near the body, it is desirable to study this inner flow as a viscous flow while retaining the inviscid flow assumptions in the outer region where only wave effects are likely to be important. Unfortunately, there is no simple way to specify conditions on the viscous-inviscid interface so that gravity waves can propagate across the interface without reflection or attenuation. This abstract presents recent development in the treatment of this issue (Hamilton, 2002) and demonstrates success of a novel technique.

The viscous-inviscid interface presents challenges both mathematically and numerically. Mathematically, the field equations describing the viscous flow in the inner region (Navier-Stokes equations) and the inviscid flow in the outer region (Laplace equation) are different and, in fact, have different numbers of unknown variables in each field. Computationally, it is typical to solve viscous-flow problems using a numerical technique that discretizes the entire fluid volume, while for inviscid flows, boundary-integral equation methods which discretize only the boundary of the flow are most popular and efficient. Utilization of a boundary-integral equation solution of the outer flow as a boundary condition for the inner flow presents the inherent difficulty that the inner viscous flow requires boundary conditions on a pointwise basis, while the solution of the outer inviscid flow admits only a global relation between pressure and velocity. Here the word “global” refers to the complete elliptic interaction of the behavior of one point with all other points on the interface boundary. Overcoming both of these challenges is essential to matching a viscous flow problem solved by a field-discretization method in an inner region to an inviscid flow problem solved by a boundary-integral equation method in an outer region.

Notable previous work on this problem was done by Campana and Iafrati (2001), who utilized the Euler equations to advance in time a velocity potential representing the outer inviscid flow based upon the so-

lution of the interior viscous flow. This time-stepping approach is effective for problems in which the viscous-inviscid matching interface does not pierce the free-surface, but was found to be unstable when surface waves pass across the matching interface (Yeung and Hamilton, 2002). The alternative approach presented below proves to be stable and robust.

Numerical solution of the interior viscous flow is performed here by a pseudo-spectral technique (Yeung and Yu, 2001), which is highly efficient but requires a geometry consisting of a vertical strut in a finite-depth fluid. The outer, inviscid flow is solved by a boundary-integral equation technique utilizing a free-surface Green function and spectral basis functions on a cylindrical surface which forms the inner boundary of the inviscid region, and the outer boundary of the viscous region.

## 2 Viscous-Inviscid Interaction

The technique of viscous-inviscid matching pursued here is to model the physical situation of an inviscid fluid adjoining a viscous fluid in such a manner that they do not mix. This leads to boundary conditions to be applied at the interface. Linearization of these conditions forms a rational basis for performing the matching between the viscous inner flow and the inviscid outer flow. In general, the boundary condition derivation is similar to the approach used by Wehausen and Laitone (1960) to develop linearized fluid-atmosphere boundary conditions which include the effects of gravity waves. To emphasize that the origins of the matching technique lie in the modeling of a physical situation, the development is done in dimensional variables and the results will be nondimensionalized for numerical implementation afterwards.

Figure 1 illustrates the geometry of the wave-body interaction problems to be investigated. Also diagrammed in this figure is the viscous-inviscid fluid domain decomposition, the viscous region near the body is denoted  $R_1$  and the inviscid region in the far field is region  $R_2$ .

The standard derivation of the linearized boundary conditions on a viscous fluid at the fluid-atmosphere interface ( $S_F$ ) assumes that the pressure is continuous across the interface and that the shear stress is pro-

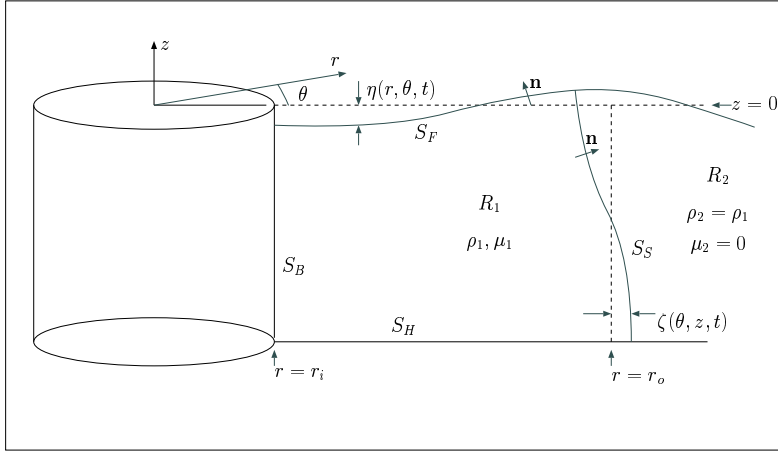


Figure 1: Schematic of viscous-inviscid interaction.

portional to the surface tension. When there is zero surface tension and a linearization is performed about the mean water level ( $z = 0$ ), these conditions result in a kinematic condition relating the wave elevation  $\eta$  to the fluid velocity vector  $\mathbf{u} = (u, v, w)$ ;

$$w(r, \theta, 0, t) = \frac{\partial \eta}{\partial t} \quad (1)$$

and three equations for the dynamic boundary condition.

$$\left. \begin{aligned} \frac{\partial w}{\partial r} + \frac{\partial u}{\partial z} &= 0 \\ \frac{\partial v}{\partial z} + \frac{1}{r} \frac{\partial w}{\partial \theta} &= 0 \\ P - \rho g \eta - 2\mu \frac{\partial w}{\partial z} &= \bar{P} \end{aligned} \right\} \text{ at } z = 0 \quad (2)$$

The boundary conditions on the viscous-inviscid interface ( $S_S$ ) are formed in a similar manner. Pressure across this interface is assumed to be continuous and it is also assumed that there is zero shear stress in the viscous fluid at the interface, consistent with the idea that the inviscid fluid presents a no-slip surface to the viscous flow. Linearization is performed about the cylindrical surface which marks the interior of the inviscid region ( $r = r_o$ ). The kinematic condition is,

$$\frac{\partial \zeta}{\partial t} = u \quad \text{at } r = r_o \quad (3)$$

where  $\zeta$  is the radial displacement of  $S_S$  and the dynamic boundary conditions are:

$$\left. \begin{aligned} P - 2\mu \frac{\partial u}{\partial r} &= \bar{P} \\ r \frac{\partial}{\partial r} \left( \frac{v}{r} \right) + \frac{1}{r} \frac{\partial u}{\partial \theta} &= 0 \\ \frac{\partial w}{\partial r} + \frac{\partial u}{\partial z} &= 0 \end{aligned} \right\} \text{ at } r = r_o \quad (4)$$

Unlike the fluid-atmosphere interface, the kinematic condition and dynamic conditions are uncoupled,  $\zeta$  does not appear in the dynamic boundary conditions as  $\eta$  does in equation (2).

### 3 Method of Numerical Solution

Having formulated the problems in the two domains, we now describe how each of the sub-problems are

solved for the special case of the interaction of waves with a vertical, circular strut. The Laplace equation describing the inviscid outer flow is solved by a boundary-integral equation method that utilizes a Green function which satisfies the linearized free-surface conditions (Wehausen and Laitone, 1960). A spectral representation of the potential on the matching surface is used and the “shell-function” techniques (Hamilton and Yeung, 2002) are used to efficiently solve the outer, inviscid flow problem. This technique is a “compute once, use many times” procedure, in which all needed Green-function evaluations are performed once for each outer region geometry. The results of this “investment” step are then stored and used to provide a linear relationship between the velocity and the velocity potential on the matching surface at each time-step for each particular outer flow. With this approach, the computational requirements of solving the outer flow become insignificant compared to the solution of the viscous interior flow.

The Navier-Stokes equations describing the viscous inner flow is solved by a pseudo-spectral field-discretization technique (Yeung and Yu, 2001). This technique is highly accurate and efficient and the only limitation is the requirement of axisymmetric geometries. However, there is no axisymmetric requirement imposed on the flow field. This method requires Dirichlet or Neumann boundary conditions on the velocity and pressure fields on all boundaries of the viscous fluid. As described in Yeung and Yu (2001), no-slip or free-slip boundary conditions are applied on the solid boundaries and linearized free-surface conditions are applied on the fluid-atmosphere interface. On the viscous-inviscid interface, a new numerical matching technique described below is applied.

### 4 Matching of Inviscid and Viscous Fields

The goal in matching the viscous and inviscid flows on the interfacial surface  $S_S$  is to ensure that the radial velocity and pressure are continuous across the matching boundary. The viscous region also requires

boundary conditions on the tangential velocities and these boundary conditions are found from the dynamic boundary conditions derived above viz. Eqn. (4). This technique is found to produce a solution in which the wave-slope is continuous across the viscous-inviscid matching boundary.

In this matching technique, the coupling between the kinematics of the flow and the dynamic boundary conditions takes place through the solution of the inviscid outer flow problem. A predictor-corrector technique is implemented that can be performed in parallel with a similar predictor-corrector procedure for advancing the fluid-atmosphere boundary conditions (1) and (2).

A boundary condition for the predicted pressure field (denoted by the overbar on the superscript) is found by inserting quantities from the previous time-step into the dynamic boundary condition on the matching surface (4),

$$P^{\bar{K}} = P_o^{K-1} + \frac{2}{Re} \frac{\partial u^{K-1}}{\partial r} \text{ at } r = r_o \quad (5)$$

where  $P_o$  is the pressure in the outer region. The Reynolds number  $Re$  is defined by  $Re = UL/\nu$  where  $\nu$  is the kinematic viscosity,  $L$  is the circular strut diameter, and  $U$  is a characteristic velocity defined by a prescribed Froude number  $Fr = \tilde{U}/\sqrt{\tilde{g}\tilde{L}}$ . The  $u^{\bar{K}}$  and  $P^{\bar{K}}$  field values are then found by solving the viscous flow equations subject to the dynamic boundary conditions (4).

At this stage, the shell-function solution of the outer flow provides a new outer pressure ( $P_o^{\bar{K}}$ ), based upon  $u^{\bar{K}}$  as a boundary condition. This solution of the inviscid flow equations subject to a Neumann boundary condition is desirable to promote a stable scheme.

Boundary conditions on the pressure field for the corrector step are computed from the predicted solution,

$$P^K = P_o^{\bar{K}} + \frac{2}{Re} \frac{\partial u^{\bar{K}}}{\partial r} \text{ at } r = r_o \quad (6)$$

The pressure field and velocity field is then re-computed everywhere by again solving the viscous flow equations.

Finally, the outer shell-function solution is used again to compute the final outer pressure based upon the final radial velocities. This procedure is similar to that used to advance the fluid-atmosphere boundary condition developed by Yu (1996), but instead of using the kinematic boundary condition on wave elevation to drive the flow, the solution of the inviscid equations of motion in the outer region performs this role.

## 5 Demonstrative Results

To demonstrate the viscous-inviscid matching, only two sets of computed results are presented, though other scenarios were also considered in Hamilton

(2002). The first case has waves originating from the collapse of a hump of fluid in the viscous region. The waves, travelling outwards, pass through the viscous-inviscid interface. Figure 2 shows the velocity and vorticity distribution of the viscous fluid at a time-step after the hump has collapsed and waves have travelled out of the viscous region. To demonstrate the effectiveness of the outer inviscid flow as a “wave absorbing” boundary, the computations are done for two cases, one at which the viscous flow extends to a radius of  $r_o = 5$  and  $r_o = 10$ . The figure shows a comparison of the two resulting flow fields, illustrating that the presence of the outer inviscid flow changes the interior viscous flow very little. In this computation, the initial wave hump had a shape described by  $\eta_o(\bar{r}) = 0.5e^{-2\bar{r}^2}$ , where  $\bar{r}$  is radius relative to a local coordinate system centered at  $(x, y) = (3, 3)$ . The Reynolds number of the viscous flow in these computations is  $Re = 5,000$ .

The second case presented in figure 3 shows the effectiveness of the viscous-inviscid matching when waves that originate in the exterior, inviscid region pass inward through the matching shell and drive the motion of the interior, viscous flow. Plane waves with a non-dimensional angular frequency of  $\omega = 1.0$  are generated by an oscillating pressure patch wave-maker (not shown) in the inviscid region and enter the viscous region from the left in figure 3. The snapshot shown is after the wavemaker has been operating for 6 periods and the flow has achieved a time-harmonic state. The solution of this problem yields viscosity-modified wave-exciting forces and moments. In the Workshop, additional results related to time history of force and moment of these and other problems will be shown.

## References

- E. F. Campana and A. Iafrati. *Proceedings of International Water Waves and Floating Bodies Conference*, 2001.
- J. A. Hamilton. PhD Dissertation, University of California at Berkeley, 2002.
- J. A. Hamilton and R. W. Yeung. *Proceedings, 21st International Conference on Offshore Mechanics and Arctic Engineering, Oslo, Norway*, 2002.
- J. V. Wehausen and E. V. Laitone. S. Flugge, editor, *Handbuch der Physik*, volume 9, pp. 446–778. Springer-Verlag, 1960.
- R. W. Yeung and J. A. Hamilton. *Proceedings, 24th Symposium on Naval Hydrodynamics, Fukuoka, Japan*, 2002.
- R. W. Yeung and X. Yu. *Hydrodynamics in Ships and Ocean Engineering, Research Institute of Applied Mechanics, Kyushu University*, pp. 87–114, April 2001.
- X. Yu. PhD Dissertation, University of California at Berkeley, 1996.

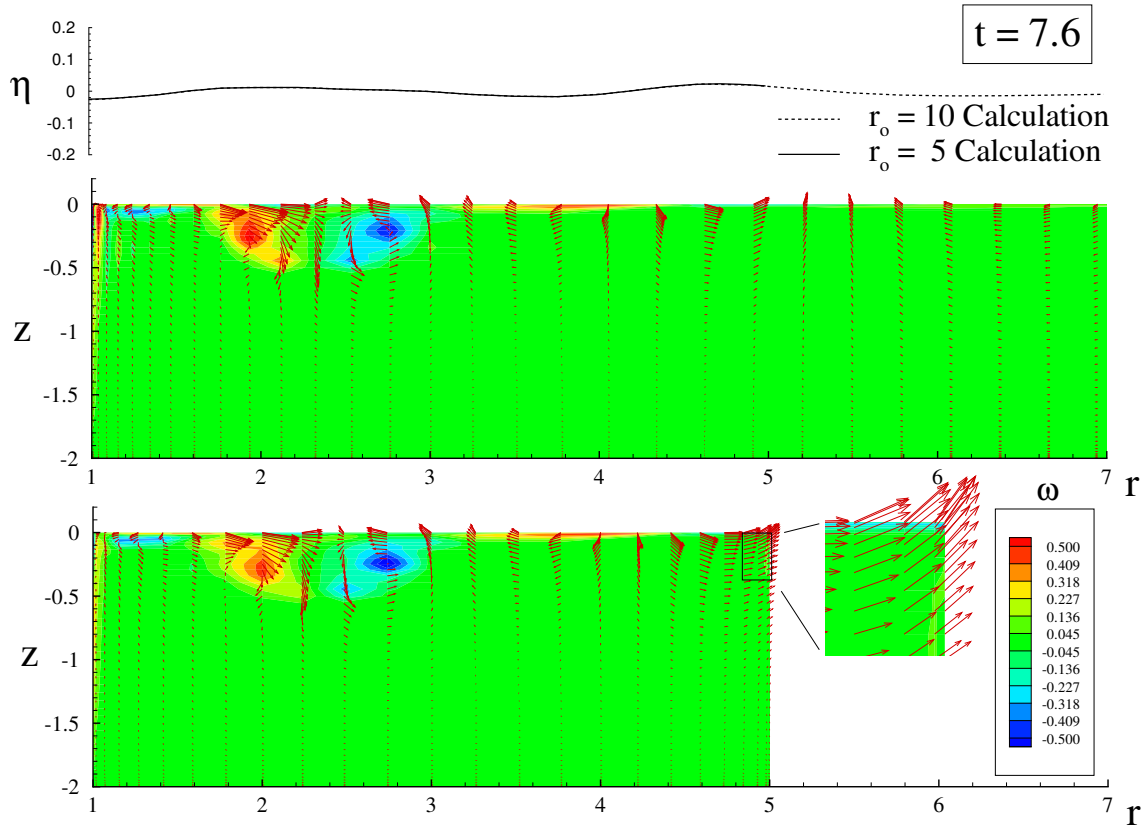


Figure 2: Comparison of velocity, the  $\theta$ -component of vorticity, and wave elevation in the  $\theta = 0$  plane at non-dimensional time 7.6 for calculations with the shell located at  $r_o = 10$  (top) and  $r_o = 5$  (bottom).

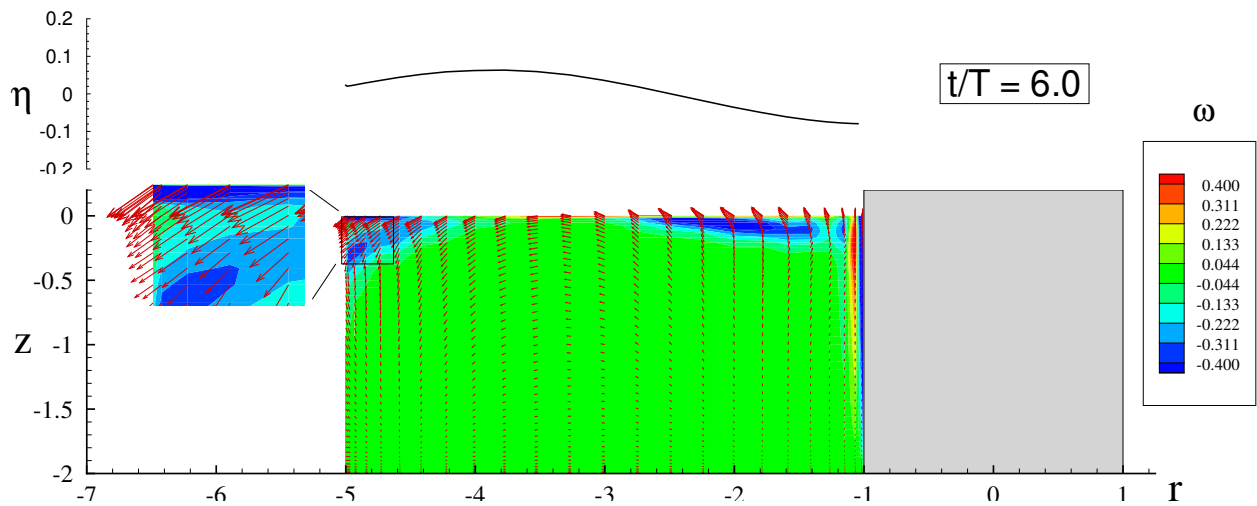


Figure 3: Velocity and  $\theta$ -component of vorticity field in the interior region due to waves generated in the outer region. This snapshot is taken after the wavemaker has oscillated for 6.0 periods.

**Question by :** H. Bingham

So far you have applied linearized conditions on the free surface; how difficult will it be to extend the method to nonlinear waves?

**Author's reply:**

Now that we have understood what are the critical variables that must be passed between the matching boundary and the manner in which that should be accomplished, both internal (viscous) flow and external (inviscid) flow can be coupled using nonlinear solution methods. The shell function formulation is actually used only for convenience to take advantage of the efficiency of linear time dependent problem, but it is not an absolute requirement in the proposed matching procedure.

---